

Article

Dynamic Quantification and Characterization of Spatial Heterogeneity in Mid-Sized Urban Landscape of India

Diksha ¹, Varun Narayan Mishra ², Deepak Kumar ³, Maya Kumari ^{4,*}, Bashir Bashir ⁵, Malay Pramanik ⁶ and Mohamed Zhran ^{7,*}

- ¹ Haryana Space Applications Centre (HARSAC), Citizen Resources Information Department CCS HAU Campus, Hisar 125004, Haryana, India; diksharana2121@gmail.com
 - ² Amity Institute of Geoinformatics and Remote Sensing (AIGIRS), Amity University Uttar Pradesh, Sector 125, Noida 201313, Uttar Pradesh, India; vnmishra@amity.edu
 - ³ Atmospheric Sciences Group, Department of Geosciences, College of Arts & Sciences, Texas Tech University, Lubbock, TX 79409, USA; deepakdeo2003@gmail.com
 - ⁴ Amity School of Natural Resources and Sustainable Development (ASNRSD), Amity University Uttar Pradesh, Sector 125, Noida 201313, Uttar Pradesh, India
 - ⁵ Department of Civil Engineering, College of Engineering, King Saud University, P.O. Box 800, Riyadh 11421, Saudi Arabia; bbashir@ksu.edu.sa
 - ⁶ Urban Innovation and Sustainability Program, Department of Development and Sustainability, Asian Institute of Technology (AIT), P.O. Box 4, Klong Luang 12120, Pathumthani, Thailand; malay@ait.asia
 - ⁷ Public Works Engineering Department, Faculty of Engineering, Mansoura University, Mansoura 35516, Egypt
- * Correspondence: mkumar10@amity.edu (M.K.); mohamedzhran@mans.edu.eg (M.Z.)

Abstract: Quantifying landscape features and linking them to ecological processes is a key goal of landscape ecology. Urbanization, socio-economic growth, political influences, and morphology have extended built-up and urban regions from the core to the boundaries. Population expansion and human activity in districts have increased outlying areas and living space borders, segmenting the urban area and affecting the local ecosystem. Current space-based remote sensing (RS) techniques could be used to visualize conditions and future prognoses for district growth to plan the infrastructure. The Land Use Land Cover (LULC) patterns in the Sonipat district, located within the National Capital Region (NCR), were examined using RS data from 2011 (Landsat 7) and 2021 (Sentinel-2) and analyzed on the Google Earth Engine (GEE) cloud platform. LULC datasets for both years were generated, followed by calculations of landscape metrics to evaluate changes across the study area. These metrics, computed using R software version 4.4.2, include analyses at three levels: five metrics at the patch level, five at the landscape level, and nine at the class level. This paper provides detailed insights into these landscape metrics, illustrating the extent and nature of landscape changes within the study area over the decade. Aggregation and fragmentation are observed in the study area, as the results indicate that urban, fallow, and barren areas have merged into larger, contiguous patches over time. This shows a consolidation of smaller patches into more extensive, connected land cover areas. Fragmentation is described as occurring between 2011 and 2021, especially in the cropland LULC class, where the landscape was divided into smaller, isolated patches. This means that larger, continuous land cover types were broken down into numerous smaller patches, increasing the overall patchiness and separation across the area, which might have an ecological impact. Landscape metrics and spatial-temporal monitoring of the landscape would aid the district council and planners in better planning and livelihood sustainability.

Keywords: LULC change; landscape metrics; fragmentation; urbanization; landscape



Citation: Diksha; Mishra, V.N.; Kumar, D.; Kumari, M.; Bashir, B.; Pramanik, M.; Zhran, M. Dynamic Quantification and Characterization of Spatial Heterogeneity in Mid-Sized Urban Landscape of India. *Land* **2024**, *13*, 1989. <https://doi.org/10.3390/land13121989>

Academic Editor: Hezi Yizhaq

Received: 26 September 2024

Revised: 5 November 2024

Accepted: 19 November 2024

Published: 22 November 2024



Copyright: © 2024 by the authors. Licensee MDPI, Basel, Switzerland. This article is an open access article distributed under the terms and conditions of the Creative Commons Attribution (CC BY) license (<https://creativecommons.org/licenses/by/4.0/>).

1. Introduction

Landscapes have changed drastically through various anthropogenic activities since the start of industrialization [1]. Urban ecosystems have supplanted natural ecosystems, and numerous alien species have been introduced [2]. Forests have diminished in number

and are now only found in highland locations with higher slopes [3]. The amount of shrubland has grown [4]. Croplands, plantation fields, and urban areas [5], among other non-native ecosystems [6], currently cover large areas, especially areas near megacities [7]. These changes are affecting native species' living conditions [8], such as the volume, distribution, and availability of resources [9], the presence of new rivals or predators, the loss of co-developed species [10], and the growth of social networks [11]. Land use is one of the most important ways that humans [12] have an impact on the environment [13]. The clearance of forest land for agricultural purposes and the establishment of communities have historically [14] been the most significant man-made land-use changes [15]. Later technological advancements in the 19th and 20th centuries [16], combined with population growth [17], increased people's need for and ability to change the environment [18] to meet their requirements; urban sprawl [19] is a major contributor to environmental degradation [20]. Spatial heterogeneity, or the diversity in physical and biological features within a landscape, is a key concept in understanding ecological health and landscape dynamics. It refers to the variation in the arrangement, size, and composition of different land elements, such as vegetation, waterbodies, and built environments, across a given area. Higher spatial heterogeneity generally supports greater biodiversity, as it provides diverse habitats and resources for various species. Conversely, lower spatial heterogeneity, often resulting from large-scale agricultural fields, urbanization, or industrial expansion, can reduce ecological resilience, making the landscape more vulnerable to environmental stressors. Understanding the landscape [21], landscape patterns, and information about features and their drivers can be improved by changing LULC [22] and modeling with spatial metrics [23]. The use of RS and geographic information systems (GIS) aids in the study of changing landscape spatial patterns [24]. The core data for landscape pattern research come mostly from categorization maps like plant, soil, and LULC maps [25]. Landscape ecologists can quickly obtain metrics for a given landscape thanks to the rapid development of GIS and RS technologies [26] and the availability of free [18] and updated software packages such as R and others [27]. Landscapes consist of a human-modified mosaic of spots, the spatial arrangement of which is referred to as a landscape pattern [28]. Landscape patterns are measured on patch, class, and landscape levels. In landscape-level surveys, patch-level metrics are quite important for giving critical information. Edges influence several species, and they are strongly related to patch interiors. This aids in the comparison of available neighborhood patches, which aids in the understanding of the patch and the degree of contrast between the patch and the surrounding area [29]. Metrics at the class level are averaged across all patches of a given type. This aids in determining how large patches contribute to the overall index. Habitat fragmentation is an example of this. Habitat fragmentation is a landscape-level process [30]. Here, it is broken down into smaller habitat fragments in metrics at the class level. This typically involves a variation in the structure and functions of the landscape composition. A single type of habitat patch, such as forest or grassland, that is demarcated in a GIS land use layer is commonly characterized as a class habitat, which is a unit between patch and mosaic [31] in landscape ecology. Because of their significant connections with numerous ecological processes, single-class spatial patterns have proven to be relevant in studies on species protection [32] and population dynamics [33]. As a result, many ecological studies [34] are interested in spatial trends at the class level. Metrics at the landscape level are the next level up in the hierarchy. These can be merged into a weighted average or used to represent aggregated patch mosaic features. The importance of landscape ecology has been influenced by this appraisal of the terrain's richness [35]. With different natural algorithms, these landscape-level measures can yield comparable or duplicate information. The amount and spatial distribution of a single patch are represented by landscape-level metrics, which can be considered as a fragmentation index [36]. As a result, it is critical to understand what kind of measure we are dealing with (patch, class, and landscape). Even though they are all relevant, changes in land use/cover are a major environmental issue that contributes to landscape fragmentation, habitat loss, and climate change [37,38]. Since the 1990s, landscape metrics have become

ubiquitous instruments for monitoring, analyzing, and planning landscape patterns, thanks to substantial improvements in landscape ecology. Landscape metrics are widely acknowledged as a helpful and significant tool for tracking, identifying, and assessing the types of changes that occur in the landscape [39]. Landscape metrics are quantitative indicators of a landscape's structural composition and spatial organization. Landscape metrics analysis is the most essential tool for studying landscape patterns and quantifying spatial variation in landscape ecology [40]. In this paper, we conduct a comprehensive analysis of landscape fragmentation in the Sonipat district by calculating landscape metrics at three distinct levels: patch, class, and landscape. These metrics encompass various landscape pattern indicators that are crucial for understanding and managing ecosystem processes. Such processes are essential for the long-term sustainability of local natural resources, particularly in regions experiencing rapid urbanization and land use changes. By combining several landscape pattern metrics, we develop a detailed typology that captures the complexities of landscape fragmentation. This typology serves as a valuable tool for evaluating and guiding policies and programs aimed at managing and maintaining the minor yet critical characteristics of the landscape. Our study provides insights into how urban expansion and population growth impact natural resources, helping policymakers and stakeholders implement more effective strategies for sustainable land management and conservation in the Sonipat district and similar rapidly developing areas.

While this study focuses on the spatial heterogeneity of the Sonipat district, the analytical approach and insights have broader applicability across diverse geographical regions and contexts. In rapidly developing areas worldwide, shifts in spatial heterogeneity often signal underlying changes in land use patterns, biodiversity, and ecological resilience. By quantifying spatial heterogeneity through metrics such as fragmentation, patch size, and edge density, this research provides a framework that can be adapted to various landscapes facing developmental pressures, from urban expansion in metropolitan regions to agricultural intensification in rural areas.

2. Study Area and Datasets

The study area, the Sonipat district, extends into the NCR (Figure 1). The Sonipat district covers an area of 2213 km² and borders the states of Delhi and Uttar Pradesh. The district is part of the Indo-Gangetic Plains, formed during the Pleistocene epoch of the Quaternary period. The elevation across Sonipat varies, with an average altitude of approximately 224 m. Sonipat's unique blend of rapid urbanization, agricultural dependency, and diverse landscape typologies within the NCR exemplifies challenges faced by many developing regions globally. Studying these dynamics allows for the generalization of findings to similarly urbanizing and agrarian areas, thereby informing sustainable land management practices across diverse contexts. In Haryana, the Yamuna River and irrigation canals flowing from it make up the district's main water supply system. The district does not have perennial rivers, and different areas have different underground water resources. The Khader area along the Yamuna has the lowest water table depth, at 10 feet. Some western and southeastern parts of the district have depths of 30 to 40 feet. Certain areas have brackish and saline groundwater. In some places, the area is not level, but overall, it is a continuous part of the Haryana–Punjab plain. The soil is fine loam with rich color throughout the district. However, some areas have sandy soil, while others have Kallar. The plain slopes gently to the south and east. The district can be divided into three distinct regions: khadar, upland plain, and sandy region. The district's climate is dry in summer and cold in winter, and the monsoon comes in July and remains until September. December marks the beginning of the winter season. The month with the lowest temperatures is January, while the months with the highest temperatures are May and June. In December, January, and February, there is light rainfall.

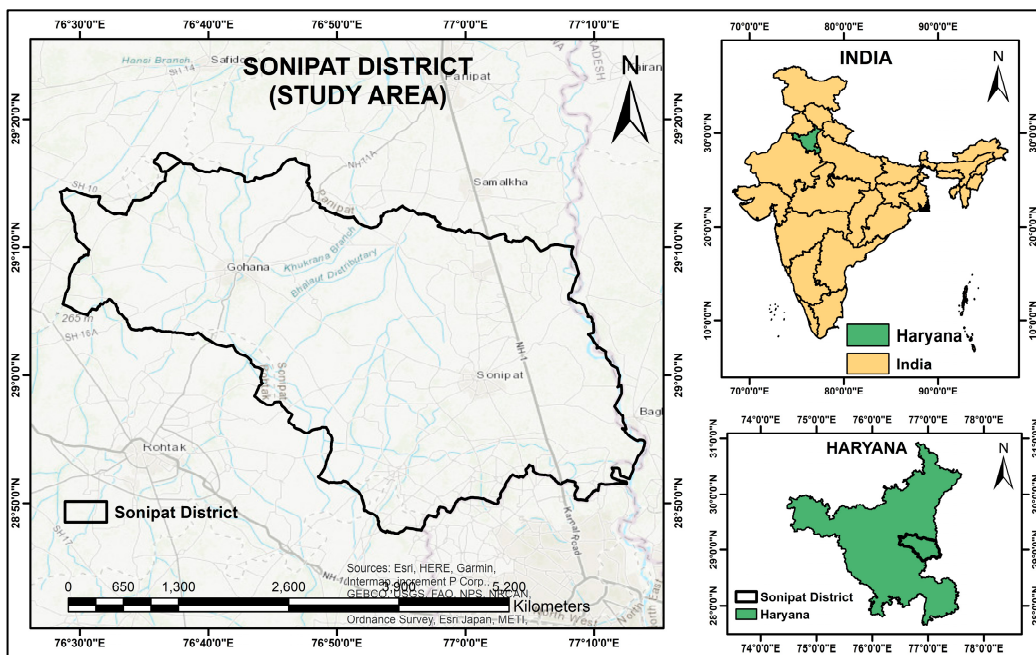


Figure 1. Geographical location of the Sonipat district.

Data Used

Two separate RS images were used in this study, taken in February 2011 (Landsat 7 image with 30 m spatial resolution) and February 2021 (Sentinel 10 m spatial resolution). The selected images have been classified as free from haze and clouds. The linear artifacts observed in the 2011 LULC map are due to the scanline corrector malfunction in the Landsat 7 satellite imagery. After the failure of Landsat 7’s scanline corrector in 2003, all subsequent images contained these distinctive linear gaps. However, these artifacts were addressed by applying standard correction techniques to reconstruct the image as accurately as possible without compromising data integrity. The corrected images maintained their overall spatial accuracy, which was essential for consistency in calculating LULC metrics. Additionally, these artifacts do not reflect any systematic bias in our analysis, as the correction techniques used ensure that these gaps did not alter or bias the spatial structure and metrics of the LULC classes in the 2011 map. A summary of the satellite data used is shown in Table 1.

Table 1. Summary of satellite data.

Datasets	Month and Year of Acquisition	Cloud Cover	Spatial Resolution	Temporal Resolution
Landsat-7 ETM+	February 2011	less than 10%	30 m	16 days
Sentinel-2	February 2021	less than 10%	10 m	5 days revised time

3. Methodology

This study aims to identify landscape metrics using RS data and GIS applications. R software was used for landscape metric measurements, and the supervised classification was carried out in GEE to create a LULC map. The software and cloud platform used for this study are listed in Table 2, and the main R packages used in this study are listed in Table 3.

Table 2. Used software and cloud platform.

Software and Cloud Platform	Script	Use	Source	Websites
Google Earth Engine (GEE)	Java	Google Cloud Platform	Open	https://code.earthengine.google.com/ , accessed on 8 October 2024
RStudio (4.1.1)	R script	Desktop	Open	https://www.rstudio.com/products/rstudio/ , accessed on 8 October 2024

Table 3. R packages used for evaluating landscape metrics.

S. No.	Packages	Description
1	landscape metrics	Landscape metrics calculation
2	raster	Spatial raster data reading and handling
3	sf	Spatial vector data reading and handling
4	dplyr	Data manipulation
5	bench	High-precision timing of R expressions

The method flow chart (Figure 2) illustrates the main steps of the general workflow, which are implemented in GEE and R. Explained below.

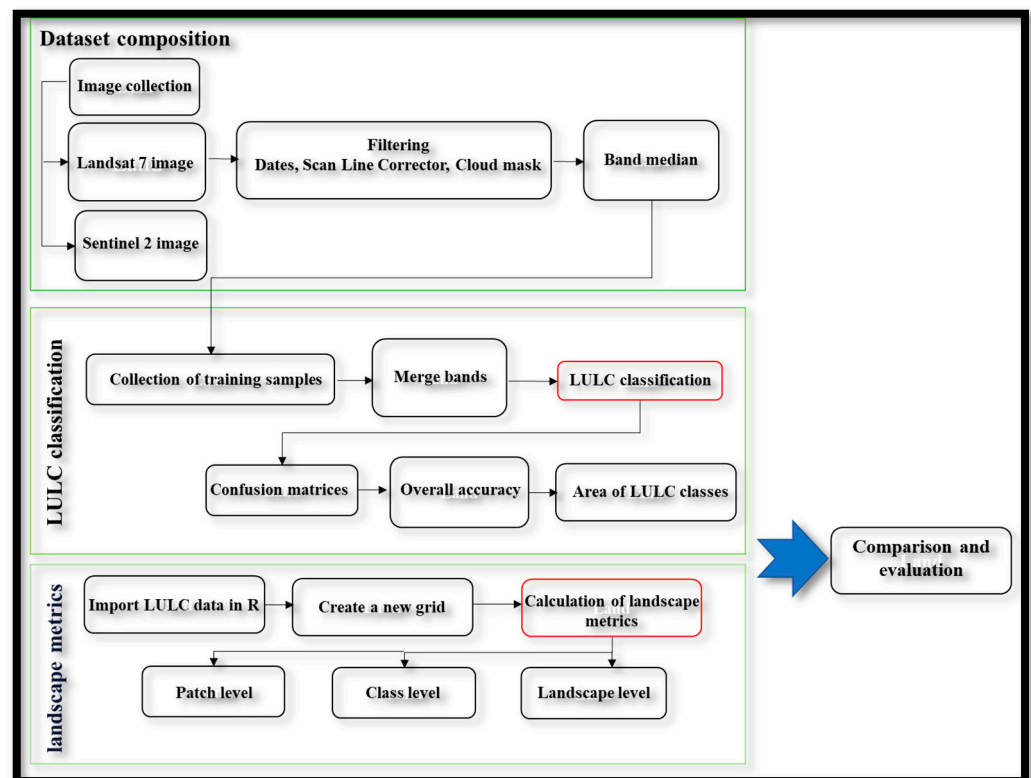


Figure 2. Methodology chart.

3.1. LULC Classification in Google Earth Engine

The landscape metrics evaluation was undertaken based on the prepared LULC map. A vital stage in every LULC classification is the preparation of the basis dataset. The creation of this dataset for the Landsat 7 and Sentinel-2 (Figure 2) data in this application begins in GEE with a filtered, cloud-masked image collection, and the median bands were computed. The LULC classification is based on a supervised technique, which, as is customary, requires gathering the essential information from the training points in order to

train the classifiers. The random forest (RF) classifier was trained and subsequently applied to the filtered, cloud-masked image collections from Landsat 7 and Sentinel-2, with median composite bands computed to optimize classification accuracy. Further, after collecting the samples and merging the class names, code running was performed, and finally, a classified map of the study area was generated, and this classified image was used for the accuracy assessments. For validation and to determine the accuracy of the classified map, training samples were taken again. For the purpose of LULC classification, four key LULC classes were identified: cropland, waterbodies, built-up, and other. Major crop-sown areas and cultivable lands were included in the layout of cropland. Natural waterbodies, small to large reservoirs, and canals were among the waterbodies. Others were fallow and barren ground, bare soil with very little flora, and drylands. Settlements, roads, railways, and industrial sites were mostly included in the built-up area. The final map layout, including legends and spatial details, was created using ArcMap 10.8 to enhance the presentation of the classified outputs.

3.2. Calculation of Landscape Metrics in R

Landscape metrics are made up of functions that calculate landscape metrics and take raster data as input. The study is primarily based on the well-known raster package. Metrics on all available levels, including patch, class, and landscape level, are included in the study. Patch-level metrics are used to describe each patch in a landscape (a patch being defined as contiguous cells belonging to the same land-cover class). All patches belonging to a specific land-cover class are described by class-level metrics. Finally, landscape-level measurements represent the landscape's overall properties. Landscape metrics can also be categorized based on the qualities of the landscape they (conceptually) describe. Shape metrics, core area metrics, aggregation metrics, diversity metrics, and complexity metrics are all examples of area and edge metrics. The script was created in R software. First, a reading of the input raster was conducted, and then a grid (50×50 cells) was created to create the boundaries of a landscape. Creating a 50×50 grid for computing landscape metrics standardizes spatial units and simplifies the analysis by dividing a complex landscape into smaller, manageable cells. This grid setup allows for a uniform approach to calculating metrics like patch density and edge length within each cell rather than across the entire landscape, making it possible to capture and interpret natural variability more effectively. A grid also maintains scale consistency, ensuring that each metric is based on an equal area size, which is crucial for comparing patterns across cells. Additionally, grids facilitate spatial analysis by providing a framework to track ecological patterns and changes systematically across space, which is essential for understanding how landscape features influence ecological processes. Using a 50×50 grid, in particular, balances detail with broader landscape coverage, enabling insights at a practical scale for multi-scale or comparative analyses. After that, an overlay was placed on the newly created grid on top of the input raster. The calculation of landscape metrics for each cell can be performed, and selected metrics specified according to the study area in the script and calculated metrics. Next, to visualize the results, values were connected to the grid. Selected metrics are discussed below in the tables.

The landscape heterogeneity was analyzed with R software. Five patch-level measures, five landscape-level measures, and nine class-level measures were selected, as shown in Tables 4–6. These measures were chosen because of their widespread usage in landscape research and well-documented effectiveness in characterizing spatial patterns. The percentage of each land cover class' area occupied in each pixel was used to determine the landscape composition of each pixel. A broader set of variables was used to quantify the landscape layout. In this study, graphical and pictorial descriptions of landscape fragmentation were compiled.

Table 4. List of patch-level landscape metrics.

Patch Level	Formula	Ranges of Change	Unit
Core area index	$CAI = \left(\frac{a_{ij}^{core}}{a_{ij}} \right) \times 100$ where a_{ij}^{core} Core area in square meters; a_{ij} Area in square meters; CAI Core area metric [41].	$0 \leq CAI \leq 100$	Percent
Euclidean nearest-neighbor distance	$ENN = h_{ij}$ where h_{ij} Distance to the nearest neighbor; ENN Aggregation metric [42].	$ENN > 0$	Meters
Fractal dimension index	$FRAC = \frac{2 * \ln * (0.25 * \rho_{ij})}{\ln a_{ij}}$ where ρ_{ij} Perimeter in meters; a_{ij} Area in square meters; FRAC Shape metric [43].	$1 \leq FRAC \leq 2$	None
Related circumscribing circle	$CIRCLE = 1 - \left(\frac{a_{ij}}{a_{ij}^{circle}} \right)$ where a_{ij} Area in square meters; a_{ij}^{circle} Area of the smallest circumscribing circle; CIRCLE Shape metric [44].	$0 \leq CIRCLE < 1$	None
Shape index	$SHAPE = \frac{P_{ij}}{\min P_{ij}}$ where P_{ij} Perimeter in terms of cell surfaces; $\min P_{ij}$ The minimum area of the patch in relation to the cell surfaces; SHAPE Shape metric [45].	$SHAPE \geq 1$	None

Table 5. List of class-level landscape metrics.

Class Level	Formula	Ranges of Change	Unit
Aggregation index	$AI = \left[\frac{g_{ii}}{\max - g_{ii}} \right] (100)$ where $AREA[patch_{ij}]$ Area of each patch in hectares; CA Area and edge metric [46].	$0 \leq AI \leq 100$	Percent
Total (class) area	$CA = \text{sum}(AREA[patch_{ij}])$ where $AREA[patch_{ij}]$ Area of each patch in hectares; CA Area and edge metric [47].	$CA > 0$	Hectares
Clumpiness index	$CLUMPY = \left[\frac{G_i - P_i}{P_i} \text{ for } G_i < P_i \& P_i < 0.5; \text{ else } \frac{G_i - P_i}{P_i} \right]$ where g_{ii} Number of like adjacencies; g_{ik} Number of all neighborhoods by class, including the focus class; $mine_i$ Minimum size of the overall class based on the cell areas, assuming complete clumping; P_i Proportion of the landscape occupied by each class; CLUMPY Aggregation metric [48].	$-1 \leq CLUMPY \leq 1$	None

Table 5. Cont.

Class Level	Formula	Ranges of Change	Unit
Core area percentage of landscape	$CPLAND = \left(\frac{\sum_{j=1}^n a_{ij}^{core}}{A} \right) * 100$ where a_{ij}^{core} Core area in square meters; A Total landscape area in square meters; $CPLAND$ Core area metric [49].	$0 \leq CPLAND < 100$	Percentage
Landscape division index	$DIVISION = \left(1 - \sum_{j=i}^n \left(\frac{a_{ij}}{A} \right)^2 \right)$ where a_{ij} Area in square meters; A Total landscape area in square meters; $DIVISION$ Aggregation metric [48].	$0 \leq Division < 1$	Proportion
Edge density	$ED = \frac{\sum_{k=1}^m e_{ik}}{A} * 10,000$ where e_{ik} Total edge length in meters; A Total landscape area in square meters; ED Area and Edge metric.	$ED \geq 0$	Meters per hectare
Normalized landscape shape index	$nLSI = \frac{e_i - \min e_i}{\max e_i - \min e_i}$ where e_i Total edge length in cell surface; $\min e_i$ $\max e_i$ Minimum and maximum total edge length in cell surfaces; $nLSI$ Aggregation metric.	$0 \leq nlsi \leq 1$	None
Perimeter-area fractal dimension	$PAFRAC = \frac{2}{\beta}$ where β Slope of the regression of the surface against the perimeter. (logarithm) $n_i \sum_{j_i}^n \ln a_{ij} = a + \beta n_i \sum_{j_i}^n \ln a_{ij}$; $PAFRAC$ Shape metric.	$1 \leq PAFRAC \leq 2$	None
Total (class) edge	$TE = \sum_{k=1}^M e_{ik}$ where e_{ik} Edge lengths in meters; TE Area and edge metric; Total (class) edge includes all edges between class i and all other classes k .	$TE \geq 0$	Meters

Table 6. List of landscape-level landscape metrics.

Landscape Level	Formula	Ranges of Change	Unit
Aggregation index	$AI = \left[\sum_{i=1}^m \left(\frac{g_{ii}}{\max - g_{ii}} \right) p_i \right] (100)$ where g_{ii} Number of like adjacencies; $\max - g_{ii}$ Classwise maximum number of like adjacencies; p_i Proportion of landscape compromised. AI Aggregation metric.	$0 \leq AI \leq 100$	Percent

Table 6. Cont.

Landscape Level	Formula	Ranges of Change	Unit
Contagion	$CONTAG = 1 + \frac{\sum_{q=1}^{nd} p_q \ln(p_q)}{2 \ln(t)}$ where p_q Adjacency table for all classes divided by the sum of that table; t Number of classes in the landscape; CONTAG Aggregation metric.	$0 < Contag \leq 100$	Percent
Disjunct core area density	$DCAD = \left(\frac{\sum_{i=1}^m \sum_{j=1}^n n_{ij}^{core}}{A} \right) * 10,000 * 100$ where n_{ij} Number of disjunct core areas; A Total landscape area in square meters; DCAD Core area metric.	$DCAD \geq 0$	Number per 100 hectares
Edge density	$ED = \frac{E}{A} * 10,000$ where E Total landscape edge in meters; A Total landscape area in square meters; ED Area and Edge metric.	$ED \geq 0$	Meters per hectare
Marginal entropy	Measures a diversity of the landscape classes.	None	log2

4. Results and Discussion

4.1. LULC Classification

The maximum region of the study area is covered by cropland, which is 83% of the total study area, although between 2011 and 2021, cropland declined from 83% to 72% of the total area. This declining trend is shown in Table 7 and Figure 3a,b.

Table 7. Area covered by different classes in the Sonipat district in 2011 and 2021.

Land Use Land Cover (LULC) Sonipat District					
LULC Classes	Area_km ² 2011	Frequency 2011	Area_km ² 2021	Frequency 2021	Change
Urban and Built-Up	234.80	11%	319.87	14%	3% Increase
Waterbodies	22.81	1%	30.55	1%	1% Constant
Cropland	1843.60	83%	1595.10	72%	11% Decrease
Other	112.14	5%	267.84	12%	7% Increase
Total	2213.37	100%	2213.37	100%	

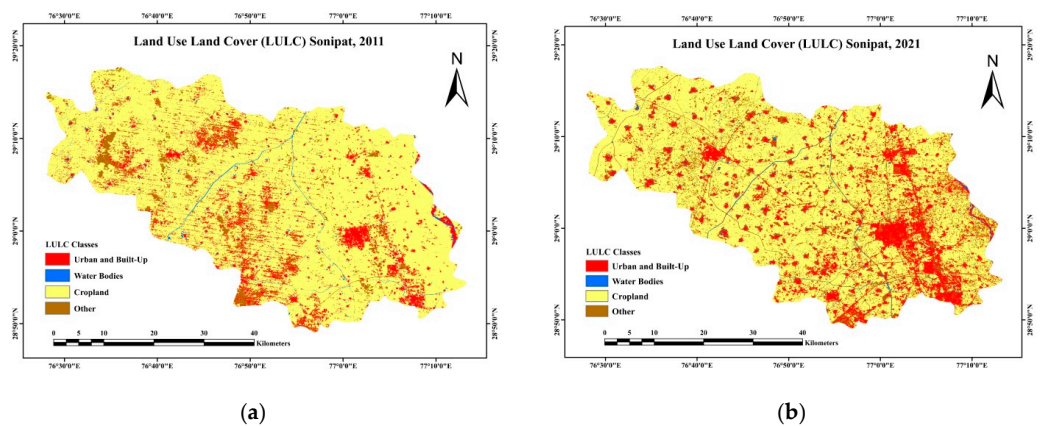


Figure 3. LULC map of Sonipat district, (a) 2011, (b) 2021.

The study area comes under the NCR, and year by year, the influence of India's capital, i.e., Delhi, can be seen in this region. Due to several developmental activities like industrialization, construction work, and an increase in residential areas, urban and built-up areas increased in the study area from 2011 to 2021, especially the parallel development along the NH-44, where urban patches increased. The urban and built-up area in 2011 was 11%, which increased to 14% in 2021, i.e., 3%. A new expressway has been constructed to improve transportation and connectivity with the capital and to reduce traffic in the capital by diverting traffic flow to the outskirts of the capital. Fallow land and barren land classes are included in other LULC classes. Other LULC classes increased from 5% to 12% during 2011–2021. The cropland started to convert into barren land due to different activities like the development of brick factories, construction work, etc. Waterbodies remained at 1% of the study area during 2011–2021, which covered the least area among other classes. These changes are clearly visible in Figure 4.

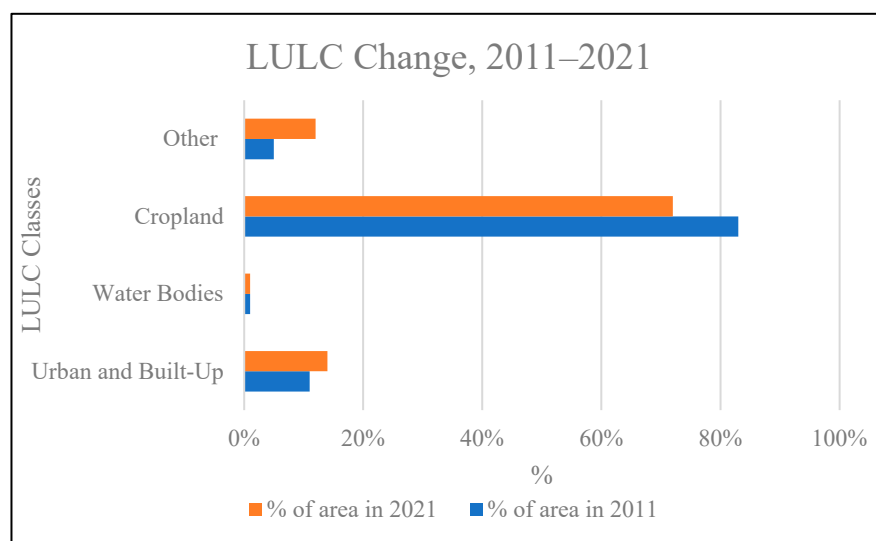


Figure 4. Percentages of the total area occupied by the LULC classes.

4.2. Sample Code for Accuracy Assessment

In this study, a confusion matrix is used to evaluate the accuracy of a classifier. The sample code in Figure 5 is used to validate data from a Landsat 7 and Sentinel-2 reference image. The results of the validation error matrix and overall validation accuracy are shown in Figure 6. The overall accuracy of the classified maps was 0.98 in both years.

```
var validationData = ValBuiltup.merge(ValWaterbody).merge(ValCropland).merge(ValOther);
print(validationData);
var bands = ['B1', 'B2', 'B3', 'B4', 'B5', 'B6', 'B7'];

var validation = clipped.select(bands).sampleRegions({collection: validationData, properties: ['Landcover'], scale: 30});
var validated = validation.classify(classifier);

//get confusion matrix
var testAccuracy = validated.errorMatrix('Landcover', 'classification');
print('validation error matrix: ', testAccuracy);
print('validation overall accuracy: ', testAccuracy.accuracy());
```

Figure 5. Sample code for computing accuracy assessment in the Sonipat district.

```

validation error matrix:
[[16,0,0,0],[0,15,0,0],[0,0,14,0],[1,0,0,14]]
0: [16,0,0,0]
1: [0,15,0,0]
2: [0,0,14,0]
3: [1,0,0,14]

validation overall accuracy:
0.9833333333333333

validation error matrix:
[[30,0,0,1],[0,14,0,0],[0,0,18,0],[0,0,0,22]]
0: [30,0,0,1]
1: [0,14,0,0]
2: [0,0,18,0]
3: [0,0,0,22]

validation overall accuracy:
0.9882352941176471
    
```

2011

2021

Figure 6. LULC classification accuracy assessment.

4.3. Landscape Metrics

4.3.1. Patch Level

- CAI:** The core area index indicates what percentage of a patch is made up of the core region. The CAI values range from 0 to 100, where 0 indicates no core area, and 100 indicates a core area. Here, when values increase from 0 to 100, it indicates increasing values in different variables and vice versa. In the study area during 2011–2021, the values of CAI ranged almost identically in waterbodies (7.69, 8.48), cropland (23.01, 23.48), and other classes (4.31, 6.02). However, in 2021, the urban and built-up class values (11.90) increased, as shown in Figure 7. The urban land patches [50] grew larger. This increase in the CAI for urban and built-up areas reflects the rapid urbanization occurring in the NCR, indicating a significant transformation of the landscape. As urban land patches expand, they encroach upon surrounding areas, potentially leading to habitat fragmentation and altered ecological dynamics. These changes underscore the need for effective urban planning and land management strategies to mitigate negative impacts on the environment. The results align with findings from [51], which reported similar patterns of urban growth and its implications for landscape ecology.

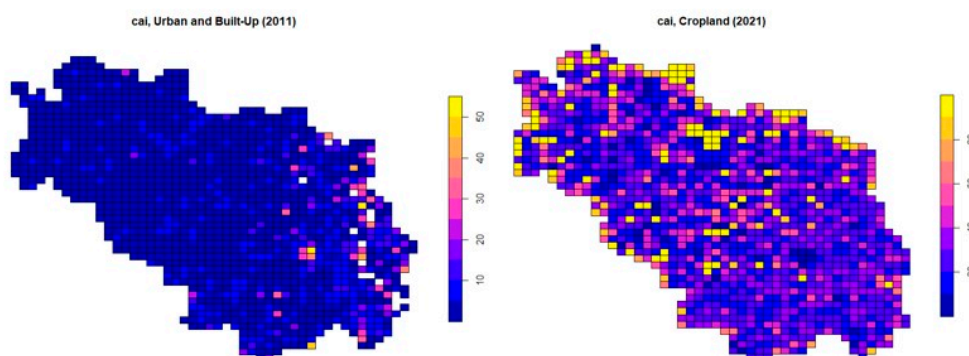
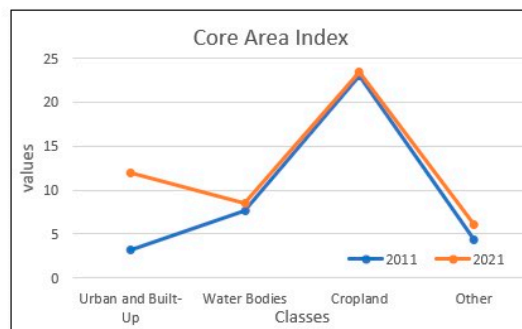


Figure 7. Graphical and pictorial representation of the highest and lowest values of a CAI, patch-level landscape metric.

- CIRCLE:** A related circumscribing circle metric is the ratio of the patch area to the patch's smallest circumscribing circle [52]. The diameter of the patch connecting the opposite corner points of the two farthest cells equals the diameter of the smallest circumscribing circle. The value ranges from 0 to 1, where 0 indicates the circular patch, and 1 indicates the linear patch. Here, values increase from 0 to 1. This indicates the changing pattern in given variables, i.e., from circular to linear and vice versa. Figure 8 shows that the urban and built-up class had the lowest value (0.50) in 2011, and the other class showed the highest value (0.55). Fragmentation occurred in 2021 because the values of the classes increased except for waterbodies. The increase in values across most classes by 2021, particularly for cropland and other land uses, signifies a transition from circular to more linear configurations. This shift highlights the fragmentation of the landscape, driven by urban expansion and the encroachment of development on previously contiguous patches. The decrease in waterbodies indicates their relative stability amidst increasing fragmentation elsewhere. Similar studies, such as those by [53], have documented these trends, emphasizing the interconnectedness of urbanization and land use changes in shaping ecological patterns.

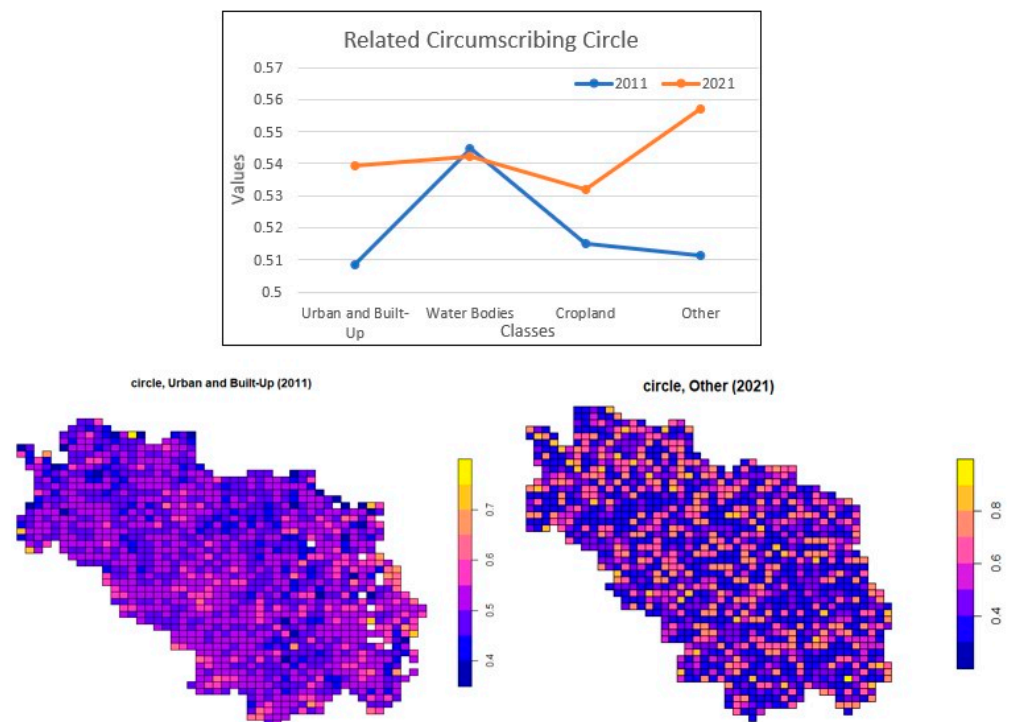


Figure 8. Graphical and pictorial representation of the highest and lowest values of a CIRCLE, patch-level landscape metric.

- ENN:** ENN shows the distance between the patch and the nearest patch of the same class. The value range starts at zero and goes to unlimited. Here, when value ranges are equal to zero, the distance to the neighbor is the least, but when it increases above zero, it shows the more isolated patches. The lowest nearest-neighbor values of 2021 suggest that the distance to the nearest neighbor is decreasing, as compared to the values from 2011. Figure 9 shows that the patches were more isolated in 2011 than in 2021.

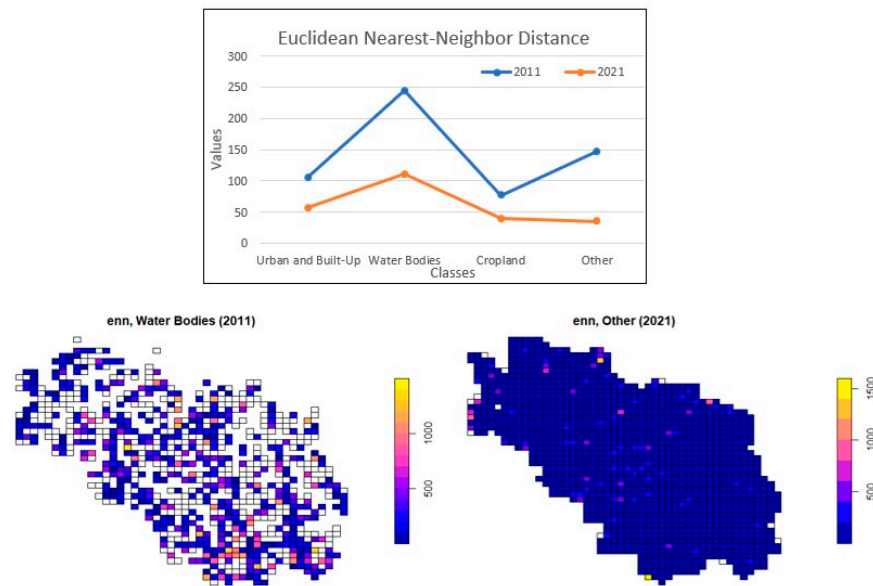


Figure 9. Graphical and pictorial representation of the highest and lowest values of an ENN, patch-level landscape metric.

- SHAPE:** The shape index value ranges from 1 and increases without limits. When values increase above 1, the patch shape becomes more complex. The values of the study area indicate that all values increase without limit. Since the patch shape of the landscape was more complex in 2011, the values of some classes, such as waterbodies (1.29) and cropland (1.47), decreased in 2021 (Figure 10).

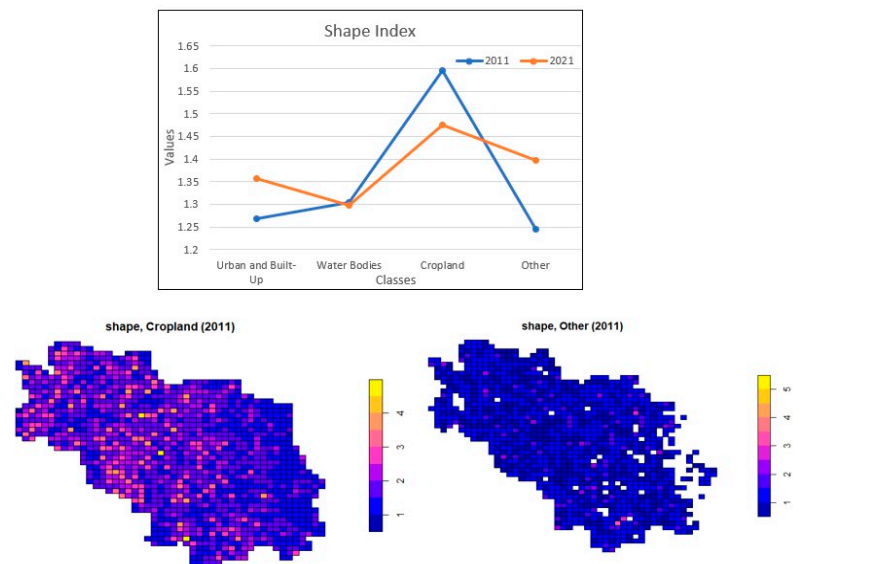


Figure 10. Graphical and pictorial representation of the highest and lowest values of a SHAPE, patch-level landscape metric.

- FRAC:** The patch complexity is described by FRAC, which is based on the patch perimeter and patch area. Here, the range remains between 1 and 2, where 1 indicates the squared patch, and 2 indicates the irregular patch. When the range moves toward 2 from 1, it tends to indicate irregular patches. The results show that the landscape of the study area has an irregular patch shape in both years, as the values increase in each LULC class shown in Figure 11. The lowest and highest values were observed in other classes in both years, 2011 (1.04) and 2021 (1.07).

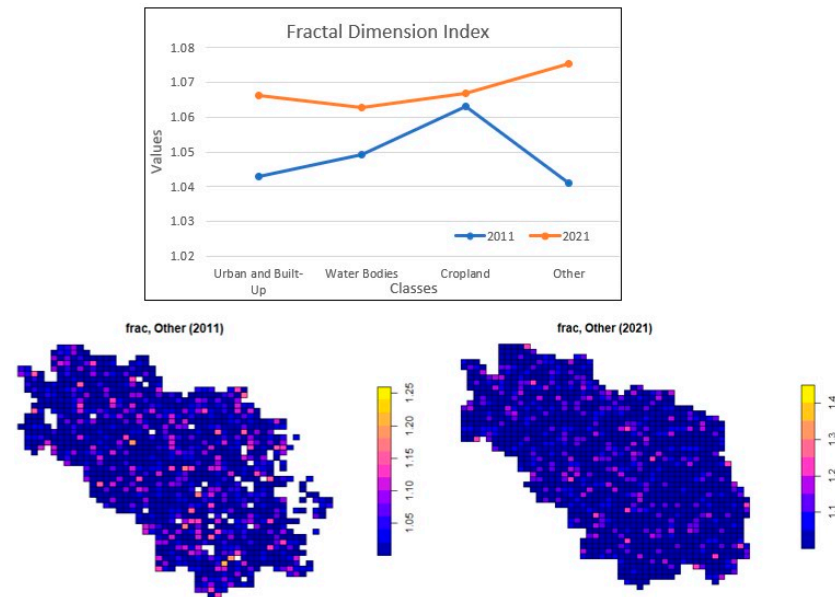


Figure 11. Graphical and pictorial representation of the highest and lowest values of a FRAC, patch-level landscape metric.

4.3.2. Class Level

- **CA:** The total area of all patches in the corresponding land class is the class area. This metric was used to calculate all class patches. Here, the range starts at 0 and increases without limit; 0 indicates the patch area of the class, and when it increases from 0, it indicates the decreasing size of the patch area. However, when it increases without limits, the patch area becomes larger. Figure 12 shows the largest cropland area (135.40) in 2011 and the lesser waterbodies area (2.52) in 2021.

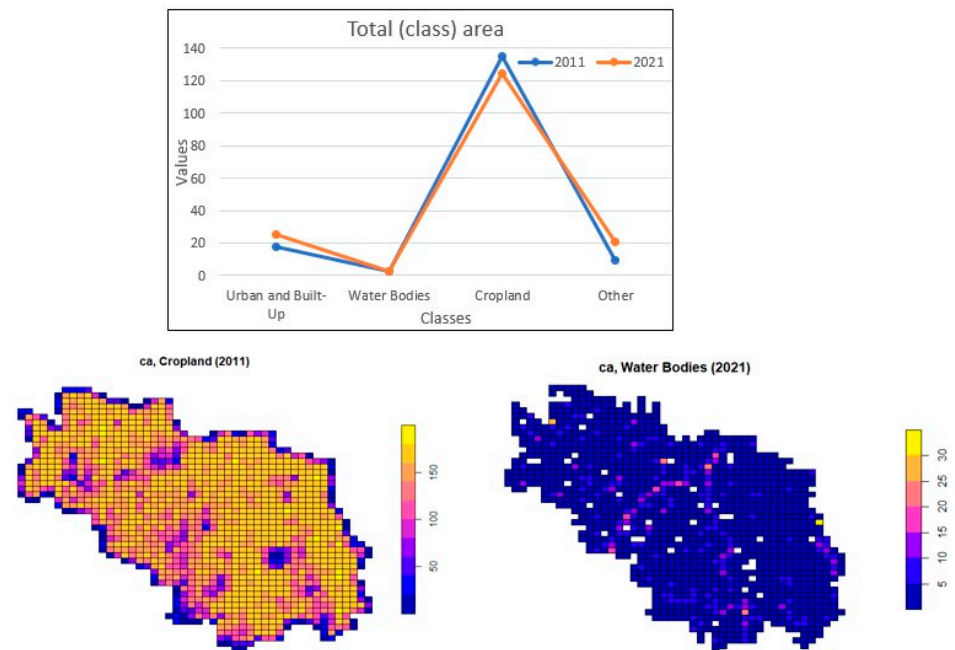


Figure 12. Graphical and pictorial representation of the highest and lowest values of a CA, class-level landscape metric.

- **Aggregation index (AI):** This index measures the district’s aggregation. The higher the value of the AI, the more aggregated it is, and the lower the value, the more disaggregated it is. Here, the range lies between 0 and 100; 0 indicates the maximum

disaggregated class, and 100 indicates maximally aggregated classes. Figure 13 depicts the fact that cropland patches were compact or aggregated in nature in both years, but fragmentation occurred in the landscape with lower values, implying urban patch desegregation in 2011. Finally, in 2021, small fragmented areas in waterbodies were observed, and in 2011, small fragmented patches were observed in other classes.

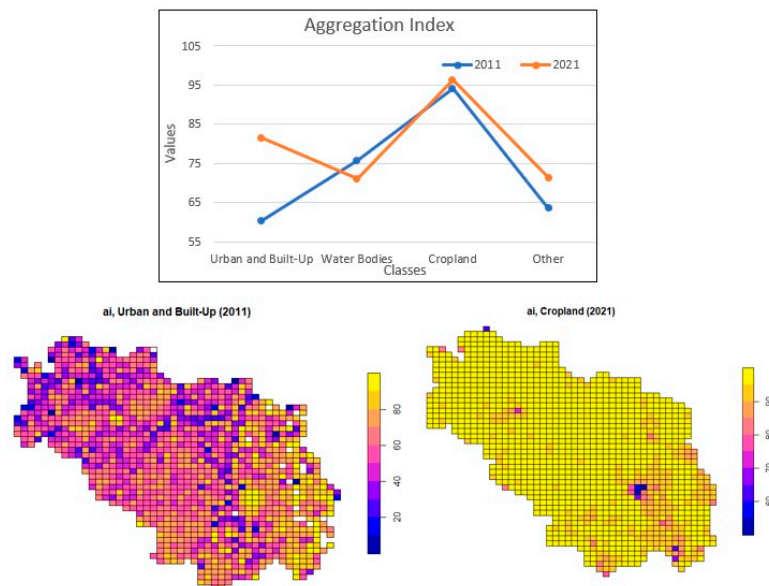


Figure 13. Graphical and pictorial representation of the highest and lowest values of an AI, class-level landscape metric.

- CLUMPY:** The aggregation of class patches is estimated by CLUPMY. CLUMPY has a range of -1 to 1 , where -1 indicates maximally disaggregated, 0 indicates randomly distributed, and 1 indicates maximally aggregated classes. In this study, cropland was more aggregated in 2021 with a value of 0.87 , whereas the value increased from 2011 to 2021 (0.66 – 0.87), indicating disaggregation or fragmentation, as shown in Figure 14.

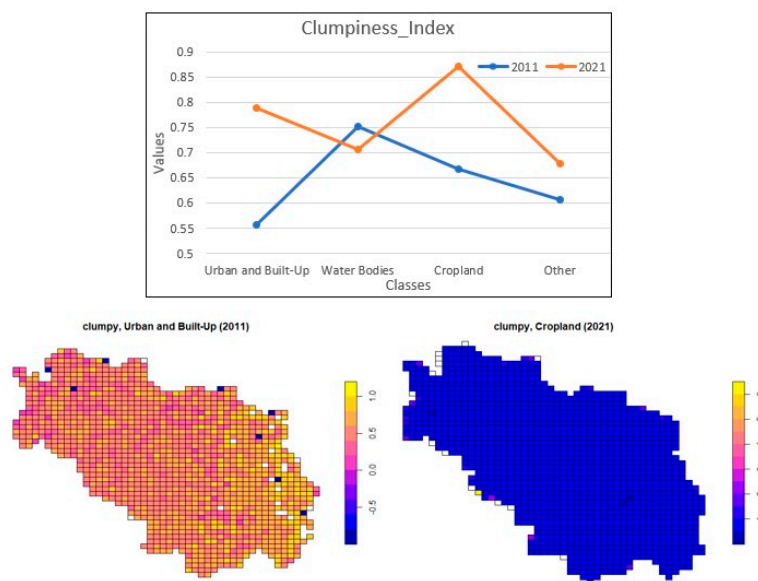


Figure 14. Graphical and pictorial representation of the highest and lowest values of a CLUMPY, class-level landscape metric.

- ED:** ED is also used to assess the fragmentation and spatial heterogeneity of the landscape. Here, the range starts at 0 and increases without limits; 0 denotes that only one patch is present (and the landscape boundary is not included), and it increases without limits, indicating that the landscape has become patchier. During the study period of 2011–2021, the value of edge density was higher in barren and fallow land (124.87) than in the other classes that compute the level of fragmentation. In 2021, compact or clumped urban growth experienced relatively higher values (74.78) in urban and built-up class areas, as shown in Figure 15.

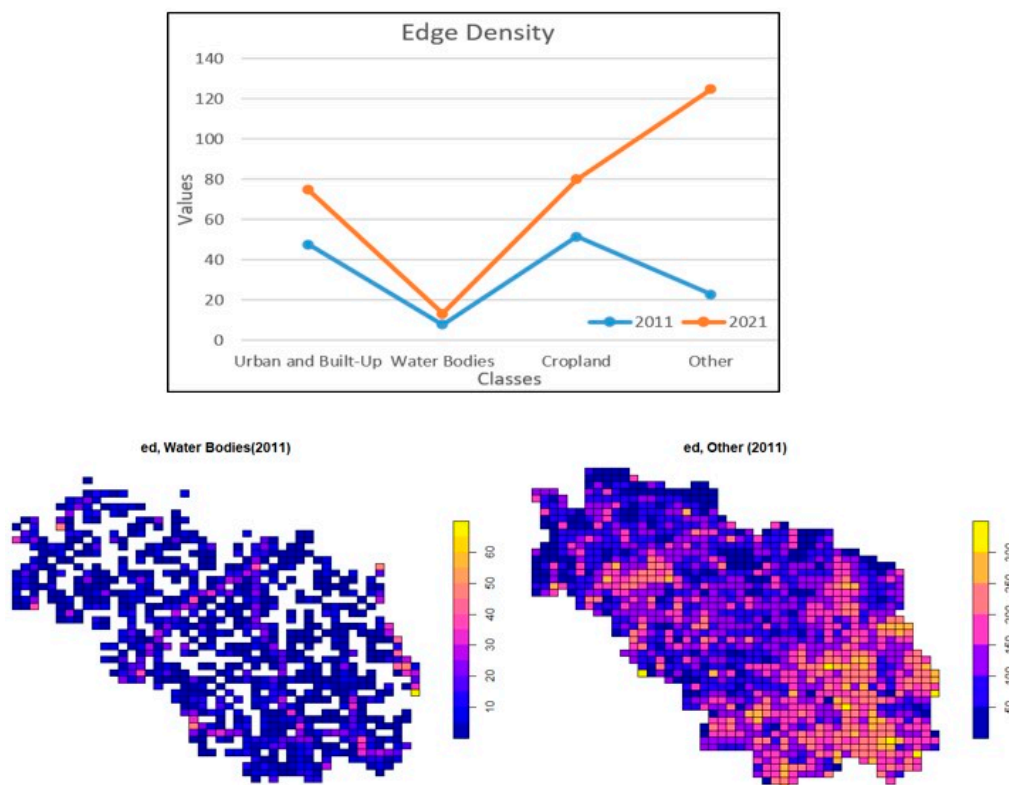


Figure 15. Graphical and pictorial representation of the highest and lowest values of an ED, class-level landscape metric.

- DIVISION:** Division is a metric for aggregation. It can be defined as the probability that two randomly selected cells are not in the same class patch. The landscape division index has a negative relationship with effective patch size. Here, the range starts at 0 and goes to 1. Here, 0 indicates only one present patch, which means equally divided cells, and 1 indicates that all patches of the class are single cells, which means approaching division. Cropland is close to zero in both years in Figure 16 because it is the dominant class in the study area.

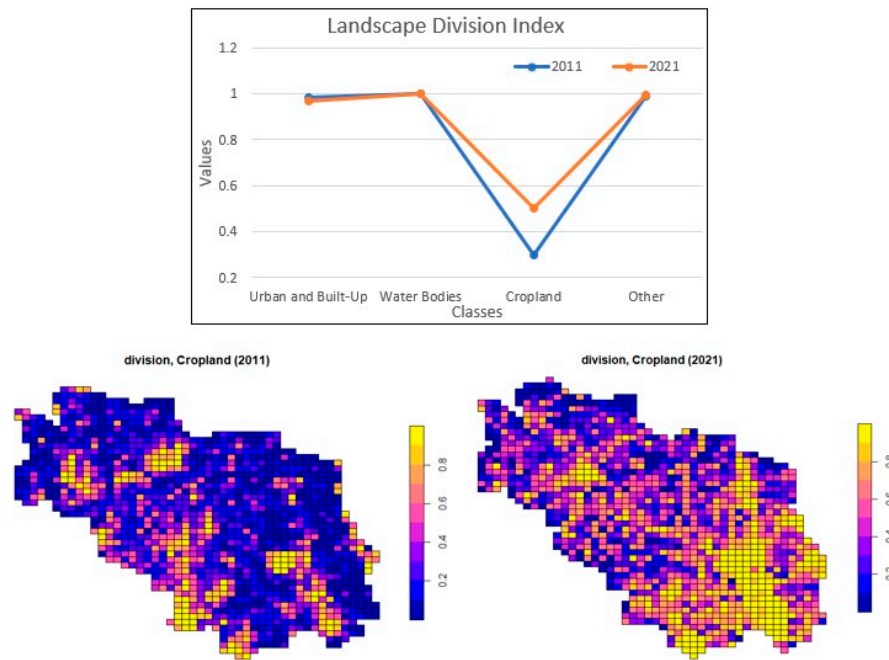


Figure 16. Graphical and pictorial representation of the highest and lowest values of a DIVISION, class-level landscape metric.

- CPLAND:** CPLAND is the percentage of the class core area in relation to the total landscape area. The value of CPLAND lies between 0 and 100, as 0 indicates all patches, and it increases toward 100, indicating patches that are larger while being rather simple in shape. The PLAND values show a growth trend in the urban and built-up classes over the last decade. The higher percentage growth of built-up area (8.90%) from 2011 to 2021 is shown in Figure 17.

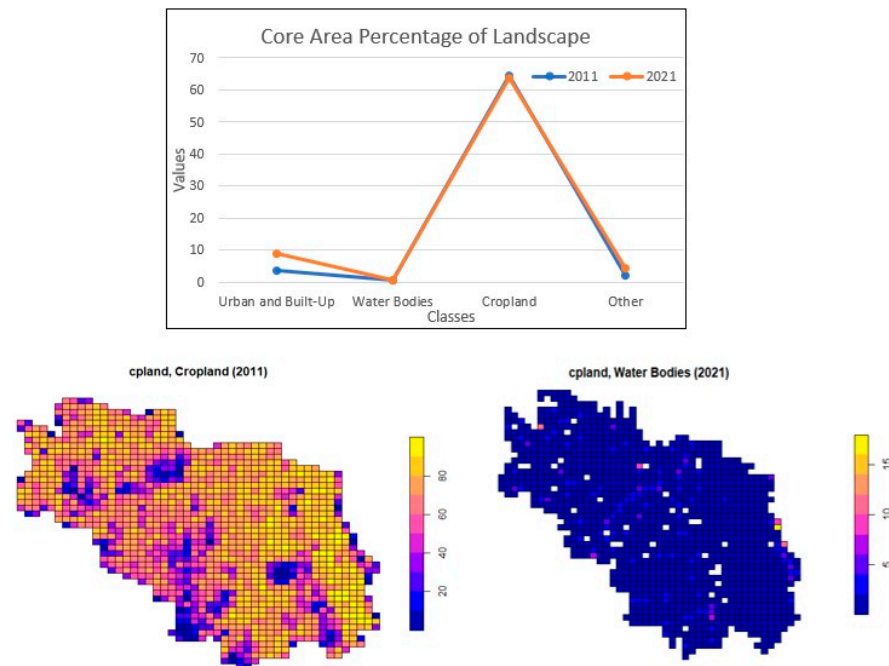


Figure 17. Graphical and pictorial representation of the highest and lowest values of a CPLAND, class-level landscape metric.

- NLSI:** NLSI is a metric for aggregation. It has a lot in common with the landscape shape index. NLSI values lie between 0 and 1; 0 indicates only one squared patch, and 1 indicates the maximum disaggregated patch. When the value increases from 0 to 1, disaggregation increases. Patches that are closer to zero are compact, while those that are further away from zero are disaggregated (Figure 18). The NLSI quantified the district's compactness with lower values in 2021, but the value was higher in 2011, indicating landscape fragmentation and disaggregation in all classes.

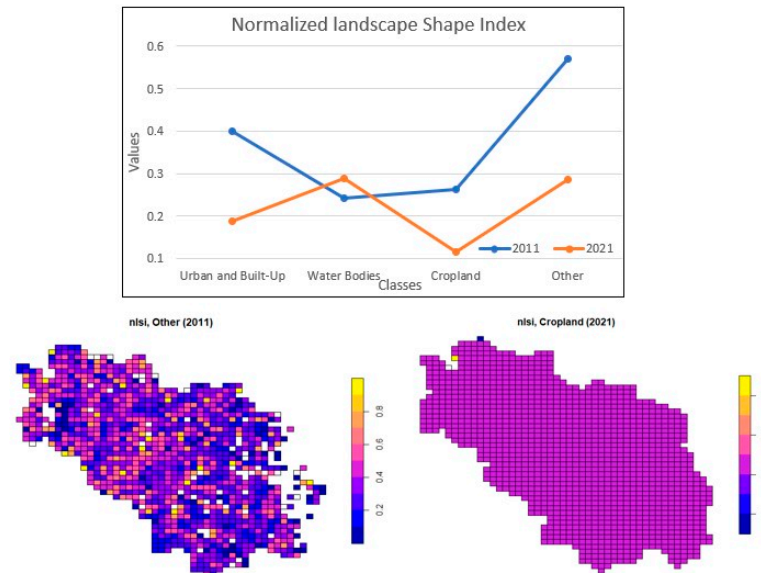


Figure 18. Graphical and pictorial representation of the highest and lowest values of an NLSI, class-level landscape metric.

- TE:** The TE metric is an area and edge metric. The value of TE starts at 0 and increases without limit; 0 indicates all cells are edge cells, and 1 indicates the landscape has become more fragmented. When the value increases, the landscape starts to become fragmented. Figure 19 shows that the study area is highly fragmented, and the landscape has many edges. All values that increased in 2021 show more fragmentation in the Sonipat district.

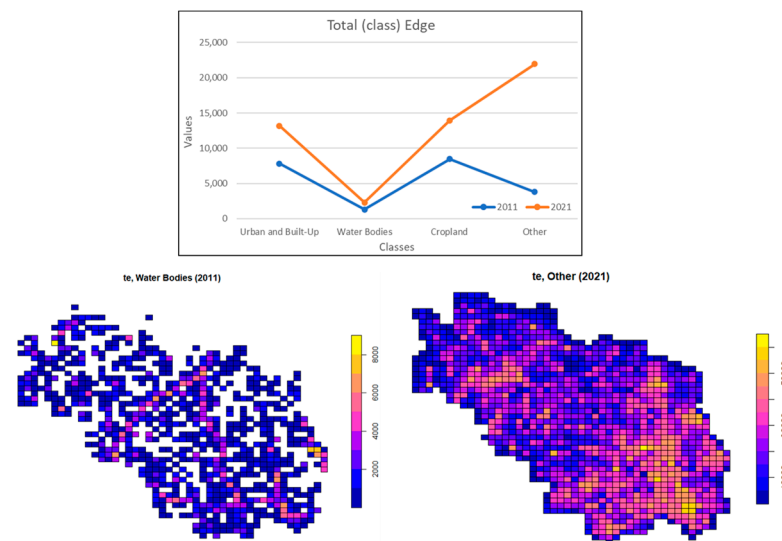


Figure 19. Graphical and pictorial representation of the highest and lowest values of a TE, class-level landscape metric.

- **PAFRAC:** PAFRAC describes the patch complexity of the class. Here, the values lie between 1 and 2, where 1 indicates patches with simple shapes, and 2 indicates patches with irregular shapes. Where values increase from 1 to 2, shapes begin to become irregular. PAFRAC results show that patches of other classes (1.41) are irregular in shape, and cropland (1.26) has simple-shaped patches in 2021, as shown in Figure 20.

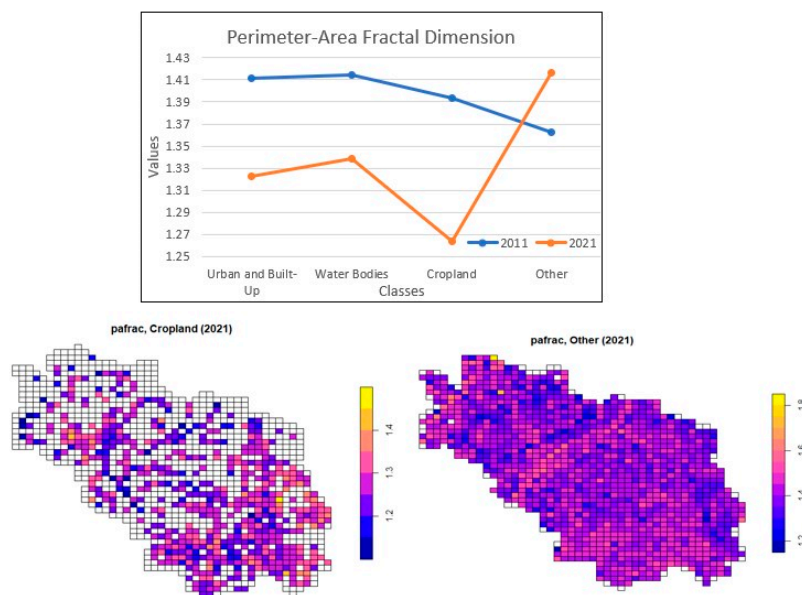


Figure 20. Graphical and pictorial representation of the highest and lowest values of a PAFRAC, class-level landscape metric.

4.3.3. Landscape Level

- **AI:** The landscape's configuration is measured by AI. The values lie between 0 and 100; 0 indicates maximally disaggregated classes, and 100 indicates maximally aggregated classes. When the value increases from 0 to 100, maximally aggregated classes begin to develop. Figure 21 and Figure 26 depict a fragmented landscape with many edges. AI values for both years are nearly identical.
- **CONTAG:** CONTAG was used to measure the landscape structure at the landscape level. Here, values lie between 0 and 100; 0 indicates that all cells are unevenly distributed, and 100 indicates that all cells are equally adjacent to all other classes. CONTAG values in 2011 were 69.94 and 65.19 in 2021, as shown in Figure 22 and Figure 26, which describe the cells of the classes as being equally adjacent to all other classes in the landscape, but the values are reduced in 2021 because the study area is degrading, on average.
- **DCAD:** DCAD is a core area metric. DCAD values lie below 0, and 0 indicates that no patch contains a disjunct core area. It increases without limit as disjunct core areas become more present, i.e., patches become larger and less complex. Figure 23 and Figure 26 show that patches of the study area become larger because the DCAD values increased in 2021 (44.86), as there are more disjoint core areas in 2021 than in 2011.
- **ED:** ED is a metric that measures both area and edge. Here, values lie above 0 and increase without limits; 0 indicates only one patch, and when they increase above 0 without limit, the landscape becomes patchier. The edge density corresponds to the density of edges in the landscape in relation to the area of the landscape. Metrics describe the configuration of the landscape. The edge density of the landscape is increased so that the landscape of the study area was patchier in 2021 than in 2011, as shown in Figure 24 and Figure 26.
- **ENT:** The ENT assesses landscape class diversity (thematic complexity). The calculated marginal entropy of the measured landscape ranges from 0.642376459 (2011) to 0.97

(2021), as shown in Figures 25 and 26. This directly implies that the complexity of the landscape is more complex in 2021.

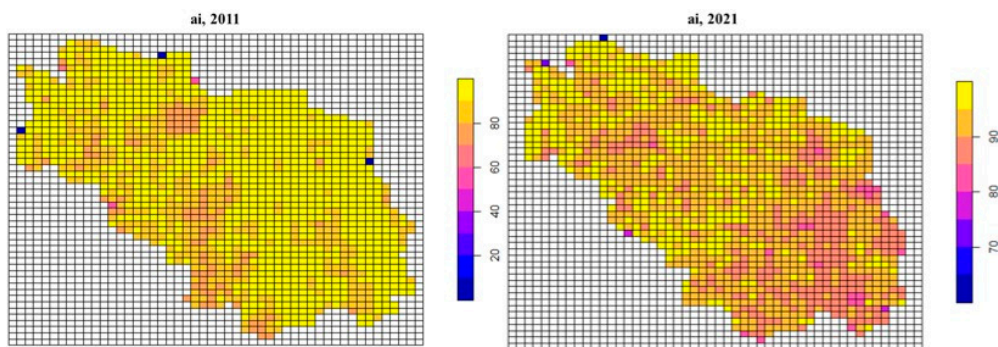


Figure 21. Pictorial representation of an AI landscape-level landscape metric.

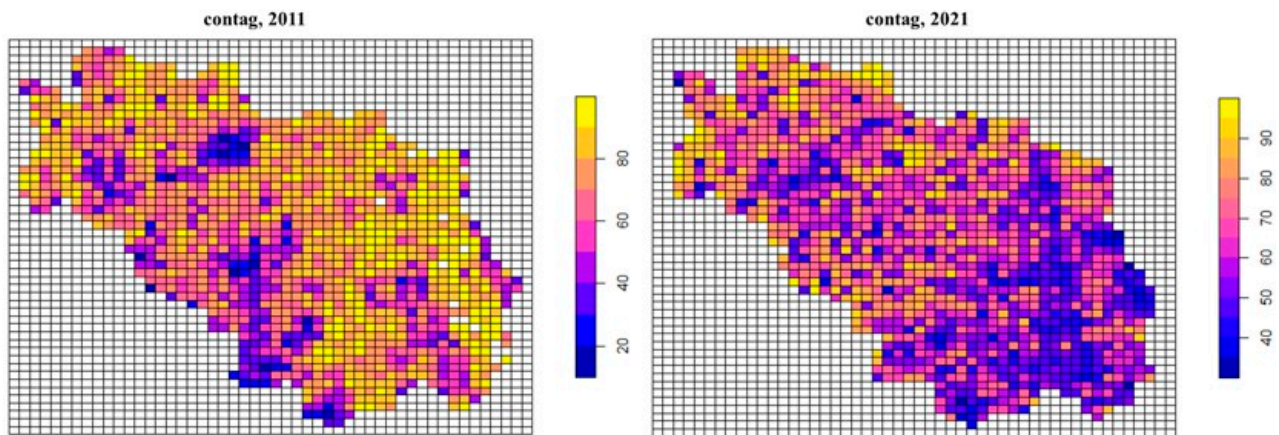


Figure 22. Pictorial representation of a CONTAG, landscape-level landscape metric.

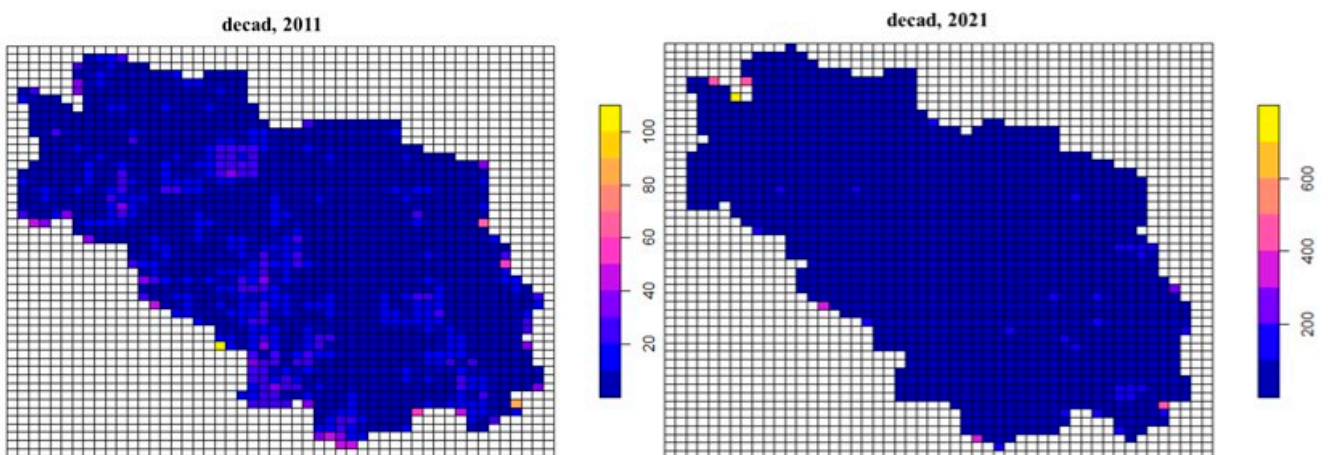


Figure 23. Pictorial representation of a DECAD, landscape-level landscape metric.

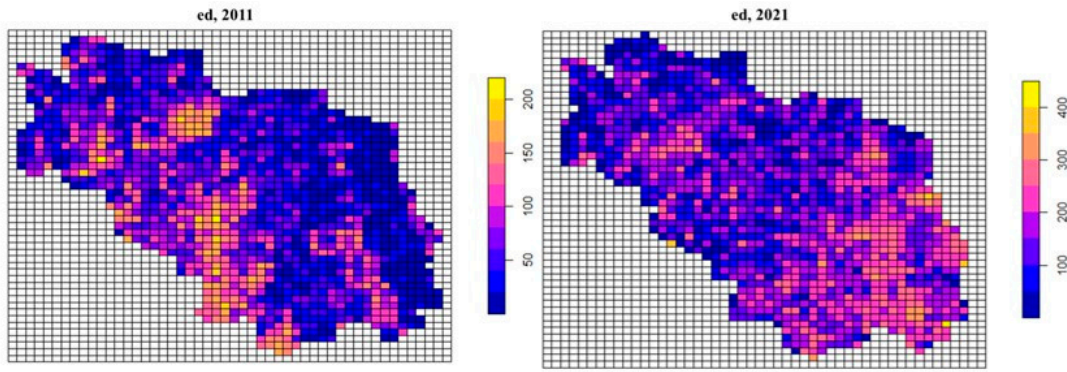


Figure 24. Pictorial representation of an ED, landscape-level landscape metric.

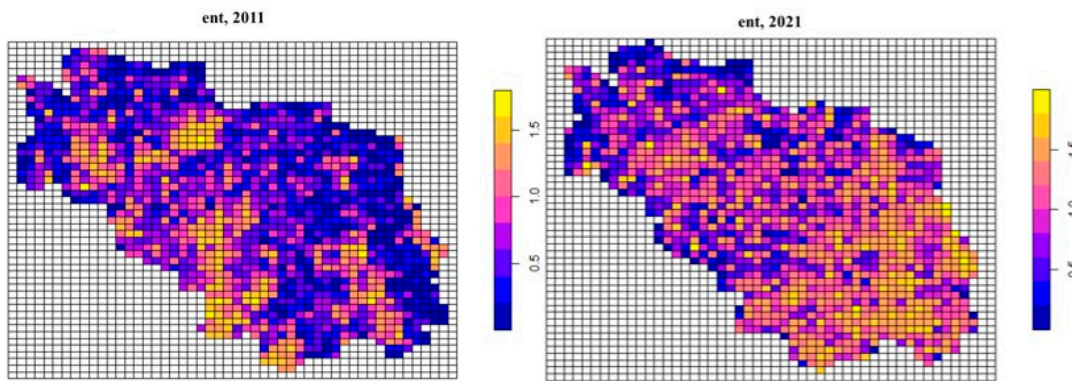


Figure 25. Pictorial representation of an ENT, landscape-level landscape metric.

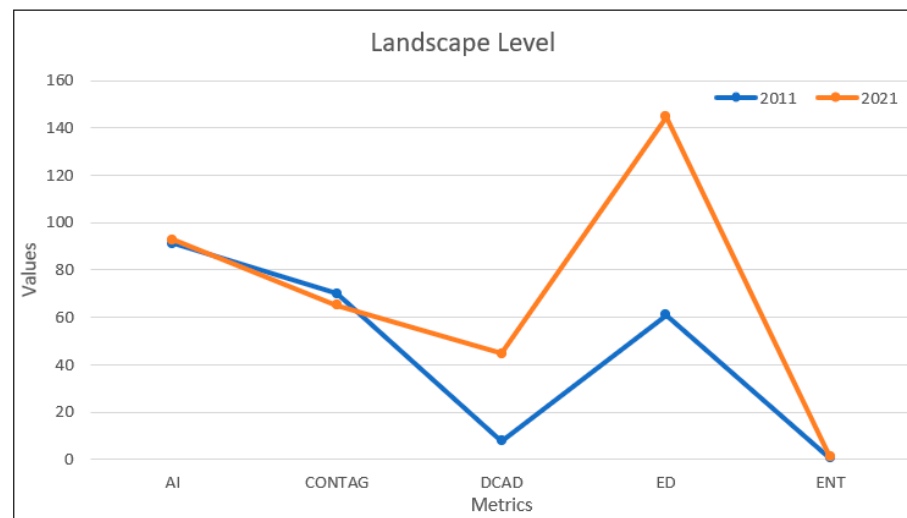


Figure 26. Graphical representation of the results of a landscape metric at landscape level.

All metrics indicate that landscape degradation and fragmentation are based on observable shifts toward reduced spatial heterogeneity, which are influenced by specific developments in the study area. Figure 27 illustrates that large agricultural patches have been fragmented due to infrastructure expansion, including the construction of canals, new road networks, and industrial zones. This leads to increased barren and fallow land patches and a notable rise in urban and built-up areas. While fragmentation can sometimes contribute to biodiversity by creating ecotones, in this context, it indicates a decline in agricultural continuity and habitat connectivity. The transformation from contiguous cropland to smaller, disconnected patches disrupts the traditional agricultural landscape

and increases the likelihood of habitat fragmentation, especially in the eastern part of the study area. Therefore, the observed fragmentation is less about ecological enrichment and more about land use changes that compromise landscape integrity and spatial continuity.

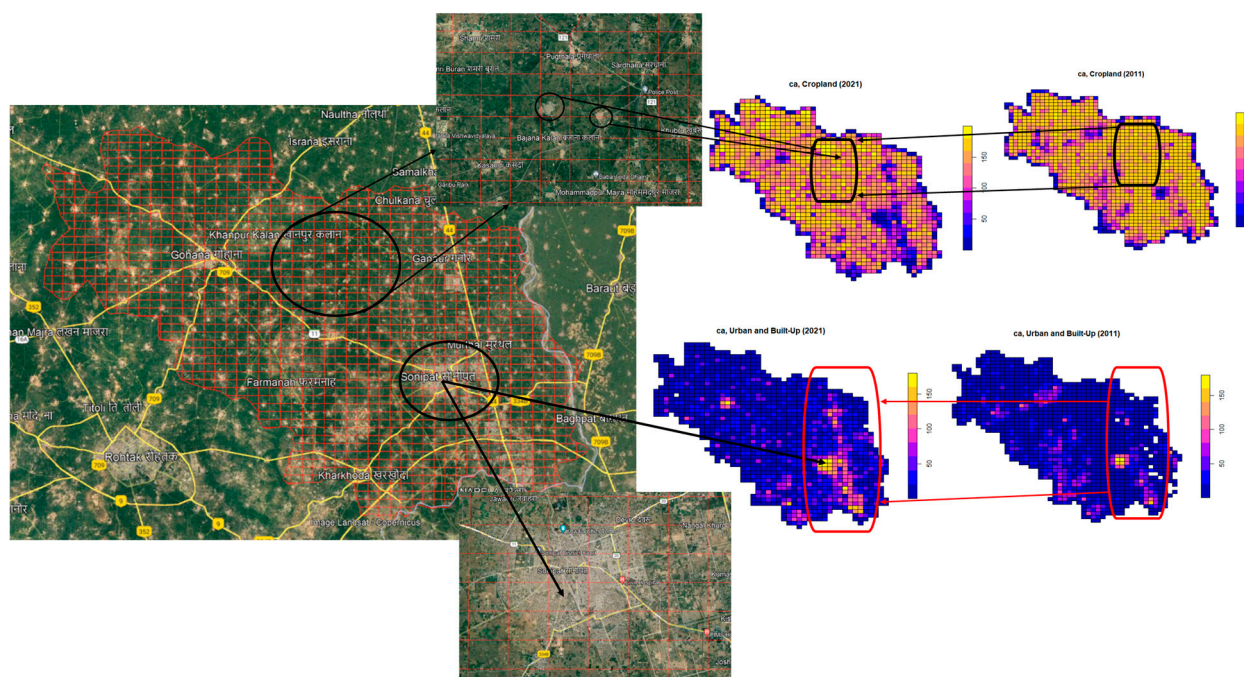


Figure 27. Area and perimeter changes in the class of cropland & urban and Built-up from 2011 to 2021.

The observed changes in the landscape structure across patch, class, and landscape levels highlight the critical importance of taking proactive measures to prevent further degradation. Metrics such as increased fragmentation, reduced core areas, and irregular patch shapes signal ecological stress, which, if left unchecked, could lead to the erosion of biodiversity, loss of agricultural productivity, and disruption of ecosystem services. The findings underscore the urgent need to integrate these metrics into local policy frameworks to develop targeted interventions, such as reforestation programs, sustainable agriculture practices, and the creation of ecological corridors to restore connectivity. Managing these changes effectively is essential to preserving the natural landscape and ensuring the long-term sustainability of natural resources in the Sonapat district.

As discussed in the Methodology, the 30 m (Landsat) and 10 m (Sentinel-2) raster data were harmonized to a consistent 30 m resolution, ensuring compatibility for calculating shape and edge metrics across years, specifically from 2011 to 2021. This resampling process minimizes discrepancies in spatial scale, allowing direct comparison over time. Although downscaling to a coarser resolution may cause minor edge blurring, this harmonization was essential for accurately analyzing landscape metrics without bias from differing resolutions. Figure 26 demonstrates that this approach preserved the integrity of calculated metrics, enabling the attribution of changes observed in 2021 primarily to actual landscape transformation rather than to resolution discrepancies.

The landscape's spatial and structural changes, particularly how fragmentation and patch metrics, reflect the ecological shifts within the study area. For example, the increase in edge density and decrease in patch size across cropland areas from 2011 to 2021 indicate a rise in landscape fragmentation. This fragmentation can disrupt habitat connectivity, reduce biodiversity, and create barriers to species movement, ultimately leading to ecological degradation. Furthermore, the metrics highlight a decline in spatial heterogeneity, especially in regions where urban expansion and infrastructure developments are prevalent. This loss of heterogeneity reflects reduced resilience in the landscape, as smaller, more

isolated patches provide fewer resources and habitat diversity than larger, contiguous ecosystems. Consequently, our metrics offer insights into how land use changes impact ecological stability, suggesting a trend toward increased vulnerability to environmental pressures within the study area.

5. Conclusions

In the last few decades, the NCR has experienced rapid urbanization, and the study area includes this region, raising concerns about associated environmental problems and the degradation of economic sustainability. Land change monitoring can thus contribute to better regional management and planning as well as a better understanding of the underlying socio-economic and biophysical processes that shape observed land changes in urban areas. RS from space allows for a retrospective, synoptic view of large areas. It can effectively assess land changes in urban areas in both spatial and temporal terms when used in conjunction with other spatial data technologies. Understanding and forecasting the accessibility of food resources, the amount and fragmentation of habitats for animal species, biodiversity, and the environment in landscapes all require an understanding of the heterogeneity of landscape patterns and their changes over time. Ecological and anthropogenic processes shape and change such landscape patterns. The current research investigates the effects and mechanisms of ecological processes on landscape patterns and how they change over time. We found that one of the main processes that leads to different patterns in landscapes is human land use. Using RS data and GIS techniques, we investigated the LULC phenomenon and computed landscape metrics. The main findings show that the extent of urban and built-up areas has grown significantly over time while cropland has decreased significantly, which has a negative impact on the environment, particularly from an ecological standpoint. Calculations of landscape metrics were also carried out, which can assist in revealing land change patterns in a quantitative manner. To fully capture the underlying processes behind the observed land changes, we need to include additional data, ancillary data, in situ observations, and qualitative methods. The landscape metrics used in this study were chosen based on some general measurements of land use area fragmentation, spread, and compactness. Different types of spatial patterns associated with different analysis scales necessitate specific measurements. In this study, metrics such as CAI, CIRCLE, ENN, FRAC, SHAPE, CA, CLUMPY, CPLAND, DIVISION, ED, NLSI, TE, and others indicated fragmentation. Landscape monitoring, which contributes to sustainable landscape management, would benefit from more information on the relative sensitivity of similar metrics to real land use changes over time. Finally, our research demonstrates the landscape of the Sonipat district's coupling effects of human land use. Cropland is the most common land use in the landscape, but due to urbanization, it is deteriorating. Despite the fact that urban and built-up patches have grown in recent decades, there is no uniformity among the various land cover classes. As a main conclusion, it was discovered that land use intensity is influenced by human factors such as cropland conversion to barren and built-up land, resulting in landscape heterogeneity. As a result, this study demonstrates the effects of various types of human land use on landscape heterogeneity. The observed landscape dynamics, quantified through various metrics, reveal patterns of fragmentation that, if not addressed, could significantly impact the region's ecological health and productivity. These metrics serve as essential tools to identify vulnerable areas requiring immediate attention, guiding policymakers in designing targeted strategies for conservation and land management. Implementing such measures is crucial to protecting the landscape from further erosion, maintaining biodiversity, and securing ecosystem services for future generations. Incorporating these findings into regional development plans will ensure sustainable growth while preserving the integrity of natural resources. Future research should integrate advanced remote sensing technologies with socio-economic analyses to understand the drivers of land use change in the NCR. Additionally, longitudinal studies on the impacts of urbanization on ecosystem services will inform sustainable land management practices.

Author Contributions: Conceptualization, D., M.K. and M.Z.; methodology, D.; software, D.; validation, D., V.N.M. and M.K.; formal analysis, D., V.N.M. and M.K.; investigation, D., V.N.M., D.K., M.K. and M.Z.; data curation, D. and M.K.; writing—original draft preparation, D.; writing—review and editing, V.N.M., D.K., M.K., B.B., M.P. and M.Z.; visualization, V.N.M., D.K. and M.K.; supervision, M.K. All authors have read and agreed to the published version of the manuscript.

Funding: This research was supported by the Researchers Supporting Project (Grant number RSP2024R296), King Saud University, Riyadh, Saudi Arabia.

Data Availability Statement: The data presented in this study are available on request from the corresponding author. The data are not publicly available due to privacy.

Conflicts of Interest: The authors declare that they have no conflicts of interest.

References

- Torres-Romero, E.J.; Nijman, V.; Fernández, D.; Eppley, T.M. Human-modified landscapes driving the global primate extinction crisis. *Glob. Chang. Biol.* **2023**, *29*, 5775–5787. [[CrossRef](#)] [[PubMed](#)]
- Gwate, O.; Dube, H.; Sibanda, M.; Dube, T.; Chisadza, B.; Nyikadzino, B. Understanding the influence of land cover change and landscape pattern change on evapotranspiration variations in Gwayi catchment of Zimbabwe. *Geocarto Int.* **2022**, *37*, 10016–10032. [[CrossRef](#)]
- Rana, D.; Kumari, M.; Kumari, R. Quantitative Estimation of Land Surface Temperature and Its Relationship with Land Use/Cover around Sonipat District, Haryana, India. *Eng. Proc.* **2021**, *8*, 31. [[CrossRef](#)]
- Egidi, G.; Quaranta, G.; Salvia, R.; Salvati, L.; Včeláková, R.; Cudlín, P. Urban sprawl and desertification risk: Unraveling the latent nexus in a mediterranean country. *J. Environ. Plan. Manag.* **2022**, *65*, 441–460. [[CrossRef](#)]
- Mishra, V.N.; Prasad, R.; Kumar, P.; Gupta, D.K.; Agarwal, S.; Gangwal, A. Assessment of Spatio-Temporal Changes in Land Use/Land Cover Over a Decade (2000–2014) Using Earth Observation Datasets: A Case Study of Varanasi District, India. *Iranian J. Sci. Technol. Trans. Civ. Eng.* **2019**, *43*, 383–401. [[CrossRef](#)]
- Mishra, V.N.; Rai, P.K.; Prasad, R.; Punia, M.; Nistor, M.M. Prediction of spatio-temporal land use/land cover dynamics in rapidly developing Varanasi district of Uttar Pradesh, India, using geospatial approach: A comparison of hybrid models. *Appl. Geomat.* **2018**, *10*, 257–276. [[CrossRef](#)]
- Kanianska, R. Agriculture and Its Impact on Land-Use, Environment, and Ecosystem Services. In *Landscape Ecology—The Influences of Land Use and Anthropogenic Impacts of Landscape Creation*; InTech: London, UK, 2016. [[CrossRef](#)]
- Guidigan, M.L.G.; Sanou, C.L.; Ragatoa, D.S.; Fafa, C.O.; Mishra, V.N. Assessing Land Use/Land Cover Dynamic and Its Impact in Benin Republic Using Land Change Model and CCI-LC Products. *Earth Syst. Environ.* **2019**, *3*, 127–137. [[CrossRef](#)]
- Yu, H.; Liu, X.; Kong, B.; Li, R.; Wang, G. Landscape ecology development supported by geospatial technologies: A review. *Ecol. Inform.* **2019**, *51*, 185–192. [[CrossRef](#)]
- Rana, D.; Kumar, D.; Kumari, M.; Kumari, R. *Assessing the Impact of Delhi Metro Network Towards Urbanisation of Delhi-NCR*; Springer Nature: Singapore, 2022; pp. 333–349. [[CrossRef](#)]
- Sajan, B.; Mishra, V.N.; Kanga, S.; Meraj, G.; Singh, S.K.; Kumar, P. Cellular Automata-Based Artificial Neural Network Model for Assessing Past, Present, and Future Land Use/Land Cover Dynamics. *Agronomy* **2022**, *12*, 2772. [[CrossRef](#)]
- Yadav, P.K.; Mishra, V.N.; Kumari, M.; Kumar, A.; Kumar, P.; Bhatla, R. Spatially explicit simulation and forecasting of urban growth using weights of evidence based cellular automata model in a millennium city of India. *Phys. Chem. Earth Parts A B C* **2024**, *136*, 103739. [[CrossRef](#)]
- Ojeh, V.; Yushau, A.; Usman, D. Assessment of Changes in Land Cover by Deforestation in Kurmi LGA, Taraba State, Nigeria Using Remote Sensing/Geographic Information System. *Aswan Univ. J. Environ. Stud.* **2022**, *3*, 67–87. [[CrossRef](#)]
- Rana, D.; Kumari, M.; Kumari, R. Land Use and Land Coverage Analysis with Google Earth Engine and Change Detection in the Sonipat District of the Haryana State in India. *Eng. Proc.* **2022**; *27*. [[CrossRef](#)]
- James, L.A. Impacts of Early Agriculture and Deforestation on Geomorphic Systems. In *Treatise on Geomorphology*; Elsevier: Amsterdam, The Netherlands, 2022; pp. 65–94. [[CrossRef](#)]
- Abbott, M.; Cohen, B. Australian Economic Development and Network Utilities. In *Monopoly Control*; Springer Nature: Singapore, 2023; pp. 13–44. [[CrossRef](#)]
- Diksha; Kumari, M.; Kumari, R. Spatiotemporal Characterization of Land Surface Temperature in Relation Landuse/Cover: A Spatial Autocorrelation Approach. *J. Landsc. Ecol.* **2023**, *16*, 1–18. [[CrossRef](#)]
- Diksha; Kumari, M.; Mishra, V.N.; Kumar, D.; Kumar, P.; Abdo, H.G. Unveiling pollutants in Sonipat district, Haryana: Exploring seasonal, spatial and meteorological patterns. *Phys. Chem. Earth Parts A B C* **2024**, *135*, 103678. [[CrossRef](#)]
- Somvanshi, S.S.; Kumari, M.; Sharma, R. Spatio-temporal analysis of rural–urban transitions and transformations in Gautam Buddha Nagar, India. *Int. J. Environ. Sci. Technol.* **2024**, *21*, 5079–5088. [[CrossRef](#)]
- Lausch, A.; Herzog, F. Applicability of landscape metrics for the monitoring of landscape change: Issues of scale, resolution and interpretability. *Ecol. Indic.* **2002**, *2*, 3–15. [[CrossRef](#)]

21. Kumari, M.; Somvanshi, S.; Sharma, R.; Zubair, S. Analysis, of multi-temporal remotely sensed spectral indices influence on ecology of Singrauli sub-district, Madhya Pradesh using an ecological impact index. *Egypt. J. Remote Sens. Space Sci.* **2022**, *25*, 863–871. [[CrossRef](#)]
22. Rana, D.; Kumari, M.; Kumar, D.; Jaiswal, N. Evaluation of Diurnal Variations in Urban Surface Temperature with Earth Observations System. *J. Environ. Assess. Policy Manag.* **2023**, *25*, 2240001. [[CrossRef](#)]
23. Rana, D.; Kumari, M.; Kumari, R. Spatiotemporal Characterization of LST and Analysis of Its Spatial Dependence: A Spatial Autocorrelation Approach. *Lect. Notes Civ. Eng.* **2023**, *333 LNCE*, 11–21. [[CrossRef](#)]
24. Groom, G.; Mûcher, C.A.; Ihse, M.; Wrбка, T. Remote Sensing in Landscape Ecology: Experiences and Perspectives in a European Context. *Landsc. Ecol.* **2006**, *21*, 391–408. [[CrossRef](#)]
25. Bishop, M.P.; James, L.A.; Shroder, J.F.; Walsh, S.J. Geospatial technologies and digital geomorphological mapping: Concepts, issues and research. *Geomorphology* **2012**, *137*, 5–26. [[CrossRef](#)]
26. Mishra, V.N.; Kumar, V.; Prasad, R.; Punia, M. Geographically Weighted Method Integrated with Logistic Regression for Analyzing Spatially Varying Accuracy Measures of Remote Sensing Image Classification. *J. Indian Soc. Remote Sens.* **2021**, *49*, 1189–1199. [[CrossRef](#)]
27. Steiniger, S.; Hay, G.J. Free and open source geographic information tools for landscape ecology. *Ecol. Inform.* **2009**, *4*, 183–195. [[CrossRef](#)]
28. Laforteza, R.; Corry, R.C.; Sanesi, G.; Brown, R.D. Quantitative approaches to landscape spatial planning: Clues from landscape ecology. *WIT Trans. Ecol. Environ.* **2005**, *84*, 239–250. Available online: www.witpress.com (accessed on 6 April 2022).
29. Darr, L.; Dawson, D.; Robbins, C. Land-use planning to conserve habitat for area-sensitive forest birds. *Urban Ecosyst.* **1998**, *2*, 75–84. [[CrossRef](#)]
30. Ma, J.; Li, J.; Wu, W.; Liu, J. Global forest fragmentation change from 2000 to 2020. *Nat. Commun.* **2023**, *14*, 3752. [[CrossRef](#)] [[PubMed](#)]
31. Turner, M.G. Landscape Ecology: The Effect of Pattern on Process. *Annu. Rev. Ecol. Syst.* **1989**, *20*, 171–197. [[CrossRef](#)]
32. Murphy, D.D.; Noon, B.R. Integrating Scientific Methods with Habitat Conservation Planning: Reserve Design for Northern Spotted Owls. *Ecol. Appl.* **1992**, *2*, 3–17. [[CrossRef](#)]
33. Betts, M.G.; Forbes, G.J.; Diamond, A.W.; Taylor, P.D. Independent Effects of Fragmentation on Forest Songbirds: An Organism-Based Approach. *Ecol. Appl.* **2006**, *16*, 1076–1089. [[CrossRef](#)]
34. McGarigal, K.; Marks, B.J. *FRAGSTATS: Spatial Pattern Analysis Program for Quantifying Landscape Structure*; Gen. Tech. Rep. No. PNW-GTR-351; U.S. Department of Agriculture, Forest Service, Pacific Northwest Research Station: Portland, OR, USA, 1995; Volume 351, 122p. [[CrossRef](#)]
35. Wu, J. Landscape Ecology. In *Encyclopedia of Ecology*; Elsevier: Amsterdam, The Netherlands, 2008; pp. 2103–2108. [[CrossRef](#)]
36. Roy, A.K.; Naskar, M.; Chakraborty, T.; Neogy, S.; Datta, D. Assessing the impact of aquafarming on landscape dynamics of coastal West Bengal, India using remotely sensed data and spatial metrics. In *Remote Sensing of Ocean and Coastal Environments*; Elsevier: Amsterdam, The Netherlands, 2021; pp. 117–138. [[CrossRef](#)]
37. O’Neill, R.V.; Krummel, J.R.; Gardner, R.H.; Sugihara, G.; Jackson, B.; DeAngelis, D.L.; Milne, B.T.; Turner, M.G.; Zygmunt, B.; Christensen, S.W.; et al. Indices of landscape pattern. *Landsc. Ecol.* **1988**, *1*, 153–162. [[CrossRef](#)]
38. Verma, P.; Singh, R.; Singh, P.; Raghubanshi, A.S. Urban ecology—Current state of research and concepts. *Urban Ecol.* **2020**, *3*–16. [[CrossRef](#)]
39. Ji, W.; Ma, J.; Twibell, R.W.; Underhill, K. Characterizing urban sprawl using multi-stage remote sensing images and landscape metrics. *Comput. Environ. Urban Syst.* **2006**, *30*, 861–879. [[CrossRef](#)]
40. Yu, M.; Huang, Y.; Cheng, X.; Tian, J. An ArcMap plug-in for calculating landscape metrics of vector data. *Ecol. Inform.* **2019**, *50*, 207–219. [[CrossRef](#)]
41. Wang, X.; Blanchet, F.G.; Koper, N. Measuring habitat fragmentation: An evaluation of landscape pattern metrics. *Methods Ecol. Evol.* **2014**, *5*, 634–646. [[CrossRef](#)]
42. Akin, A.; Erdoğan, M.A.; Berberoğlu, S. The Spatiotemporal Land use/cover Change of Adana City. *Int. Arch. Photogramm. Remote Sens. Spat. Inf. Sci.* **2013**, *XL-7/W2*, 1–6. [[CrossRef](#)]
43. Wu, H.; Sun, Y.; Shi, W.; Chen, X.; Fu, D. Examining the Satellite-Detected Urban Land Use Spatial Patterns Using Multidimensional Fractal Dimension Indices. *Remote Sens.* **2013**, *5*, 5152–5172. [[CrossRef](#)]
44. Amiri, B.J.; Junfeng, G.; Fohrer, N.; Mueller, F.; Adamowski, J. Regionalizing Flood Magnitudes using Landscape Structural Patterns of Catchments. *Water Resour. Manag.* **2018**, *32*, 2385–2403. [[CrossRef](#)]
45. Hulshoff, R.M. Landscape indices describing a Dutch landscape. *Landsc. Ecol.* **1995**, *10*, 101–111. [[CrossRef](#)]
46. He, H.S.; DeZonia, B.E.; Mladenoff, D.J. An aggregation index (AI) to quantify spatial patterns of landscapes. *Landsc. Ecol.* **2000**, *15*, 591–601. [[CrossRef](#)]
47. Wang, X.; Cumming, S.G. Measuring landscape configuration with normalized metrics. *Landsc. Ecol.* **2011**, *26*, 723–736. [[CrossRef](#)]
48. Neel, M.C.; Mgarigal, K.; Cushman, S.A. Behavior of class-level landscape metrics across gradients of class aggregation and area. *Landsc. Ecol.* **2004**, *19*, 435–455. [[CrossRef](#)]
49. Shao, S.; Yu, M.; Huang, Y.; Wang, Y.; Tian, J.; Ren, C. Towards a Core Set of Landscape Metrics of Urban Land Use in Wuhan, China. *ISPRS Int. J. Geoinf.* **2022**, *11*, 281. [[CrossRef](#)]

50. Reed, D.N.; Anderson, T.M.; Dempewolf, J.; Metzger, K.; Serneels, S. The spatial distribution of vegetation types in the Serengeti ecosystem: The influence of rainfall and topographic relief on vegetation patch characteristics. *J. Biogeogr.* **2009**, *36*, 770–782. [[CrossRef](#)]
51. Schumaker, N.H. Using landscape indices to predict habitat connectivity. *Ecology* **1996**, *77*, 1210–1225. [[CrossRef](#)]
52. Riitters, K.H.; O'Neill, R.V.; Hunsaker, C.T.; Wickham, J.D.; Yankee, D.H.; Timmins, S.P.; Jones, K.B. A factor analysis of landscape pattern and structure metrics. *Landsc. Ecol.* **1995**, *10*, 23–39. [[CrossRef](#)]
53. Istanbuly, M.N.; Binesh, A.; Amiri, D.J.; Parsa, V.A.; Amiri, B.J. Unveiling the threshold in forest patch shapes to soil retention ecosystem services. *J. Environ. Manag.* **2024**, *368*, 122188. [[CrossRef](#)]

Disclaimer/Publisher's Note: The statements, opinions and data contained in all publications are solely those of the individual author(s) and contributor(s) and not of MDPI and/or the editor(s). MDPI and/or the editor(s) disclaim responsibility for any injury to people or property resulting from any ideas, methods, instructions or products referred to in the content.